Stimulated Raman scattering in lithium formate monohydrate crystals at temperatures from 2 to 300 K

K. K. Lai,* W. Schüsslbauer,† H. Silberbauer, H. Amler, U. Bogner, and Max Maier
Naturwissenschaftliche Fakultät II (Physik), Universität Regensburg, Postfach 397, D-8400 Regensburg, Federal Republic of Germany

M. Jordan and H.-J. Jodl
Fachbereich Physik, Universität Kaiserslautern, Postfach 3049, D-6750 Kaiserslautern, Federal Republic of Germany
(Received 29 December 1989; revised manuscript received 28 March 1990)

Stimulated Raman scattering in x-, y-, and z-cut lithium formate monohydrate ($LiHCOO \cdot H_2O$) crystals was studied in a resonator configuration with use of a Q-switched ruby laser. The temperature dependence of the stimulated Raman threshold intensity was measured from 2 to 300 K for different polarizations of the laser light. Stimulated Raman scattering from the 79-cm^{-1} yy $A_1(z)$ mode, the 104- or 1372-cm^{-1} zz $A_1(z)$ modes, the 76-cm^{-1} A_2 mode, or the 82-, 113-, or 163-cm^{-1} $B_1(x)$ modes was observed, depending on the propagation direction in the crystal, the polarization of the laser light, and the temperature. The results of stimulated Raman scattering are discussed using the measured temperature-dependent spontaneous Raman data from the same lattice modes. Steady-state and transient theories of stimulated Raman scattering for a broadband pump laser (ruby-laser linewidth 0.7 cm^{-1}) are applied to explain the experimental results.

I. INTRODUCTION

Lithium formate monohydrate is a solution-grown crystal[1,2] with many interesting properties. It is piezoelectric[1] and pyroelectric[3] and has high values of the electro-optic[1,4] and strain-optic[4] coefficients. The crystal has highly nonlinear optical properties. It has been used for second-harmonic,[5,6] third-harmonic,[7] and fourth-harmonic[8,9] generation from the ir to the uv spectral region (up to 230 nm) and for frequency mixing.[7,9,10] Optical phase conjugation has been studied using the lithium formate monohydrate crystal as a degenerate optical parametric amplifier.[11] Spontaneous Raman scattering[12,13] and polariton scattering[14,15] have been investigated mainly at room temperature. Galzerani *et al.*[13] have presented detailed spontaneous Raman measurements for different laser light polarizations and propagation directions in the crystal at 297, 90, and 4.2 K. The spectral resolution was not sufficient to allow the determination of the spontaneous Raman linewidths below room temperature. Parametric scattering[16] and coherent anti-Stokes Raman scattering[17] have been observed for a few selected phonon modes. Lithium formate monohydrate is an interesting crystal also for stimulated Raman scattering because large crystals of good optical quality can be easily grown from solution and because it has a high threshold intensity for optical damage[4] exceeding by far 500 MW/cm^2.

In this paper we present investigations of stimulated Raman scattering (SRS) in lithium formate monohydrate single crystals. The methods of growth and preparation of the crystals and their optical properties are described in Sec. II. The experiments were carried out with a Q-switched ruby laser with a linewidth of 0.7 cm^{-1}. The results of steady-state and transient theories of stimulated Raman scattering for a broadband pump laser are shortly reviewed in Sec. III. After a description of the apparatus in Sec. IV, the experimental results on stimulated Raman scattering in a resonator configuration are presented and discussed in Sec. V. The threshold intensity of stimulated Raman scattering was investigated as a function of temperature from room temperature to 2 K for different propagation directions in the lithium formate monohydrate crystal and different polarizations of the laser light. In addition, the spontaneous widths and intensities of those Raman lines, which were observed in SRS, were measured as a function of temperature.[18] The theoretical relations between the threshold intensity for SRS and the spontaneous Raman data presented in Sec. III are used for a discussion of the experimental results.

II. GROWTH, PREPARATION, AND PROPERTIES OF LITHIUM FORMATE MONOHYDRATE CRYSTALS

Lithium formate monohydrate is known to crystallize in the orthorhombic system [crystal class $mm2$ (C_{2v}), space group $Pbn2_1$ (C_{2v}^9)] with four molecules in the unit cell.[19] Single crystals of high optical quality and dimensions of about $20 \times 20 \times 50$ mm^3 were grown from an aqueous solution[2] by slow surface evaporation at constant temperature (42 °C) in a temperature-controlled container. The crystals were cut with a thread saw so that their faces were normal to the crystallographic axes. The crystal faces were polished with diamond paste on a lead-tin plate. Since lithium formate monohydrate is hygroscopic and tends to dehydrate,[20] the crystals were kept in a box with relative humidity between 40% and 60%.

Lithium formate monohydrate is essentially transpar-

ent from 0.25 to about 1.2 μm.[6] It is negative biaxial birefringent with the principal axes x, y, and z parallel to the crystallographic axes a, b, and c, respectively.[6] The threshold intensity for optical damage of the surfaces of our crystals was measured with a Q-switched ruby laser ($\lambda_L = 694.3$ nm, linewidth 0.7 cm^{-1}) to be about 2 GW/cm^2. This value is very high as compared with other materials used for SRS, e.g., $LiNbO_3$, which is yet damaged in the bulk with a threshold of about 500 MW/cm^2.

According to Loudon[21] the polarizability tensors $\underline{\alpha}$ for the orthorhombic $mm2$ (C_{2v}) point group of lithium formate monohydrate are given by

$$\underline{\alpha}_{A_1(z)} = \begin{bmatrix} xx & 0 & 0 \\ 0 & yy & 0 \\ 0 & 0 & zz \end{bmatrix}, \quad \underline{\alpha}_{A_2} = \begin{bmatrix} 0 & xy & 0 \\ yx & 0 & 0 \\ 0 & 0 & 0 \end{bmatrix}, \tag{1}$$

$$\underline{\alpha}_{B_1(x)} = \begin{bmatrix} 0 & 0 & xz \\ 0 & 0 & 0 \\ zx & 0 & 0 \end{bmatrix}, \quad \underline{\alpha}_{B_2(y)} = \begin{bmatrix} 0 & 0 & 0 \\ 0 & 0 & yz \\ 0 & zy & 0 \end{bmatrix}, \tag{2}$$

with $xx \neq yy \neq zz \neq xx$ and $xy = yx$, $xz = zx$, $yz = zy$.[22] All modes are Raman active and the $A_1(z)$, $B_1(x)$, and $B_2(y)$ modes are also simultaneously infrared active with electric dipole moments in the z, x, and y directions, respectively.[13]

There have been several investigations of spontaneous Raman scattering in lithium formate monohydrate.[12–15] However, the existing data are not sufficient for the discussion of our measurements of SRS, because the spontaneous Raman linewidths have not yet been determined. Therefore, we have also investigated spontaneous Raman scattering of those Raman modes which were observed in SRS, as a function of temperature. The results will be presented in detail in a forthcoming paper.[18]

III. RELATION BETWEEN THE STIMULATED RAMAN THRESHOLD INTENSITY AND THE SPONTANEOUS RAMAN DATA

For a comparison of the results of stimulated Raman scattering with the spontaneous Raman data, two different cases are distinguished: pumping with monochromatic or broadband laser pulses.

For a monochromatic laser line the situation is simple. The threshold intensity I_{th} of SRS depends on the inverse of the Raman gain factor g, which is related to the integrated scattering cross section $d\sigma/d\Omega$ and the spontaneous Raman linewidth $\delta\bar{\nu}_R$. It can be shown that the threshold intensity is given by[23]

$$I_{\text{th}} \propto \frac{1}{g} \propto \frac{\delta\bar{\nu}_R}{d\sigma/d\Omega} \propto \frac{1}{(d^2\sigma/d\omega\, d\Omega)_P}, \tag{3}$$

where $(d^2\sigma/d\omega\, d\Omega)_P$ is the peak scattering cross section in the center of the spontaneous Raman line. This equation shows that the threshold intensity is low for strong and narrow spontaneous Raman lines.

The situation is more complicated for a broadband laser line in a dispersive medium. In this case, it has been shown[24–27] that the Raman gain may depend on the spontaneous Raman linewidth $\delta\bar{\nu}_R$ and the laser linewidth $\delta\bar{\nu}_L$. A critical laser intensity I_{cr} has been introduced,

$$I_{\text{cr}} = 4\delta\bar{\nu}_L |\mu| c/(ng), \tag{4}$$

which determines the effective Raman gain. The quantity

$$\mu = \frac{1}{v_L} \mp \frac{1}{v_S} \tag{5}$$

depends on the difference (forward scattering) or sum (backward scattering) of the group velocities, v_L and v_S, of the laser and Stokes light. It is determined by the dispersion of the refractive index of lithium formate monohydrate. When the laser intensity I_L is much larger than the critical intensity I_{cr} the Raman gain is approximately equal to the monochromatic laser line case. For $I_L \lesssim I_{\text{cr}}$ the effective Raman gain is reduced and depends on the laser and spontaneous Raman linewidths.

Since we use a Raman resonator we have to consider separately the forward and backward direction, which have different critical intensities [see Eqs. (4) and (5)]. The problem in calculating the critical intensities is that the gain factors g are not known for the different Raman modes of lithium formate monohydrate. It is very difficult to determine g from the measurements of the threshold intensity I_{th} of SRS because the value of I_{th} depends on I_{cr} for forward and backward scattering. If we assume that the gain factors of the investigated Raman modes are in the range $10^{-3} < g < 10^{-2}$ cm/MW and if we use the refractive index data of lithium formate monohydrate[28] we estimate for the $B_1(x)$ modes critical intensities $34 < I_{\text{cr}}^{\text{fw}} < 340$ MW/cm^2 for forward scattering and $560 < I_{\text{cr}}^{\text{bw}} < 5600$ MW/cm^2 for backward scattering. The critical intensities for forward scattering of the other Raman modes may be lower than that of the $B_1(x)$ modes because of the smaller differences in the refractive indices; however, the actual values depend on the individual Raman gain factors. From a comparison of the estimated critical intensities I_{cr} with the threshold intensities I_{th} measured in Sec. V, it is concluded that for forward scattering from most of the investigated lattice modes the threshold intensities I_{th} are probably larger than the critical intensities $I_{\text{cr}}^{\text{fw}}$, i.e., nearly the full Raman gain is available. For backward scattering, in general, $I_{\text{th}} \lesssim I_{\text{cr}}^{\text{bw}}$, therefore the Raman gain is reduced. It should be noted that for stationary SRS Eq. (3) is also valid for broadband laser lines.

There is an additional complication which has to be taken into account. SRS may be transient or quasistationary depending on the product of the Raman linewidth $\delta\omega_R = 2\pi c\,\delta\bar{\nu}_R$ and the laser pulse duration T_L. When $\delta\omega_R T_L \gtrsim g I_L l$, then quasistationary SRS is observed.[29] I_L and l are the laser intensity and the length of the Raman medium, respectively. The threshold intensity I_{th} is then determined by the peak scattering cross section $(d^2\sigma/d\omega\, d\Omega)_P$ [see Eq. (3)]. When the spontaneous Raman linewidth is very narrow, i.e., $\delta\omega_R T_L \lesssim g I_L l$,

transient SRS occurs[29] with a smaller Raman gain and a higher threshold intensity than in the steady-state case. It has been shown,[27] that for transient SRS the threshold intensity I_{th} is given in a good approximation by

$$I_{th} \propto \frac{1}{(g\delta\bar{\nu}_R)^{1/2}} \propto \frac{1}{(d\sigma/d\Omega)^{1/2}} . \quad (6)$$

It is interesting to note that in this case the threshold intensity depends on the *integrated* scattering cross section, but is independent of the spontaneous Raman linewidth.

IV. EXPERIMENT

Stimulated Raman scattering in lithium formate monohydrate was excited by a Q-switched ruby laser. The light pulses had a duration of about 25 ns, an energy up to 1 J, a divergence of about 10 mrad, and a linewidth of 0.7 cm^{-1}. The laser light was linearly polarized. The experimental setup is shown schematically in Fig. 1. The laser power was attenuated by filters F and registered by a fast photodiode PD1. The laser light was focused with lens L1 (focal length $f_1 = 40$ cm) into the lithium formate monohydrate crystal CR which was mounted on the cold finger of a flowing gas-helium cryostat or in a liquid-helium bath cryostat. At the lowest temperature the crystal was immersed in superfluid helium. The laser light transmitted through the crystal was detected with photodiode PD2. x-, y-, and z-cut crystals with different lengths (13–23 mm) were used in the experiments. Their surfaces were polished as described in Sec. II and formed an angle of about 1°. One of the y-cut crystals was polished by Gsänger Optical Components (Planegg/Munich, Germany) with a flatness of $\lambda/50$ and an angle of less than 2″ between the surfaces.

The crystal CR was placed inside an external resonator with a length of 40 cm (see Fig. 1). The angle α between the resonator axis and the ruby-laser beam was about 1°. Mirrors $M1$ and $M2$ of the resonator had a reflectivity of about 98% at the ruby laser frequency and at the Stokes frequencies with shifts <200 cm^{-1}. The reflectivity for the Stokes light shifted by 1372 cm^{-1} was 67%. $M1$ was a flat mirror, $M2$ had a radius of curvature of 10 m. The Raman Stokes light transmitted through mirror $M2$ was focused with lens $L2$ on a ground-glass plate G in front of the entrance slit of a 60-cm grating monochromator M (see Fig. 1). The Stokes light was detected by a photodiode array PDA in the exit plane of the monochromator. The photodiode array was connected with a transient recorder. The polarization of the Stokes light could be analyzed by polarizer P.

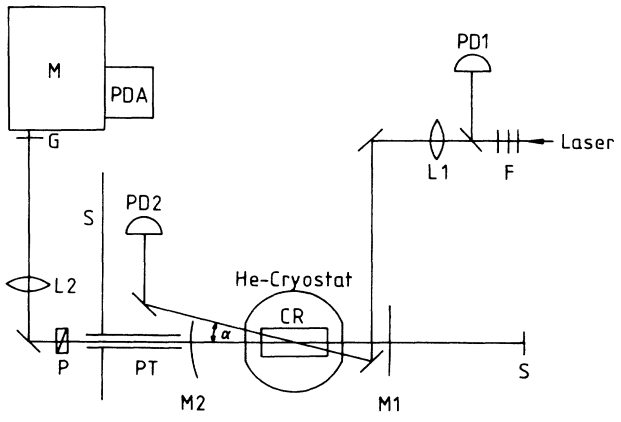

FIG. 1. Experimental setup for the excitation and detection of stimulated Raman scattering in a lithium formate monohydrate crystal: F, filters; $L1$,$L2$, lenses; PD1,PD2, photodiodes; CR, crystal; $M1$,$M2$, mirrors of the Raman resonator; P, polarizer; G, ground-glass plate; M, monochromator; PDA, photodiode array; S, beam stop; PT, paper tube.

We define the threshold intensity I_{th} for SRS as the laser intensity when the Raman-Stokes intensity becomes detectable by the photodiode array. I_{th} was calculated from the measured laser power and beam diameter (about 1 mm) in the crystal assuming Gaussian intensity distributions both over the cross section and as a function of time.

Spontaneous Raman scattering was excited by a single-mode Ar^+ laser (linewidth 0.001 cm^{-1}, power 0.5 W) using appropriate scattering geometries and oriented single crystals of lithium formate monohydrate to measure the different lattice modes of interest. The crystal, between thin indium films, was pressed via springs to the cold flange of a closed-cycle cryostat (lowest achieved sample temperature 11 K). The Raman light was investigated with high spectral resolution S_r using a conventional triple monochromator ($S_r^{Mo} \approx 0.5$ cm^{-1}) in tandem with a standard pressure scanned Fabry-Pérot interferometer ($S_r^{FP} \leq 0.01$ cm^{-1}). This idea—to improve the resolution by combining a conventional Raman spectrograph with an interferometer—goes back to Pine and Tannenwald;[30] meanwhile modified and reinvented by others in the last 20 years. After photoelectric registration the signal was stored in a multichannel analyzer and transferred to a computer.

Each Raman mode was measured several times at each temperature. The stability of the interferometer was controlled after each measurement. The spontaneous Raman linewidth was determined by deconvolution of the experimental Raman profiles assuming an airy function as the spectral apparatus function and a Lorentzian function for the Raman line shape. The frequency-integrated spontaneous Raman intensities were determined with the monochromator with large slit widths (without Fabry-Pérot interferometer). The values of the frequency shifts of the spontaneous Raman lines given in this paper were measured at room temperature against calibration lines with an accuracy of about 0.5 cm^{-1}. For more details we refer to a forthcoming paper.[18]

V. EXPERIMENTAL RESULTS AND DISCUSSION

We measured the threshold intensities I_{th} for SRS and the widths and intensities of the corresponding spontaneous Raman lines as a function of temperature for different propagation directions in the crystal and for different polarizations of the laser light. It should be noted that the measured absolute values of the threshold intensities and the competition between stimulated Raman

scattering of the different lattice modes, which are discussed in the following sections, do not only depend on the spontaneous Raman data but also on our particular experimental conditions, e.g., the reflectivities of the Raman resonator mirrors at the different Stokes frequencies, the linewidth of the ruby-laser pump pulse, the parallelism and quality of the crystal surfaces, the adjustment of the Raman resonator, etc.

A. *x* direction

In this case, the entrance and exit surfaces of the crystal were perpendicular to the x direction, which was parallel to the direction of the axis of the resonator for SRS (see Fig. 1). The ruby-laser light propagated in the xy or xz plane with its **k** vector forming a small angle α (about 1°) with the x direction.

1. z polarized laser light

For linearly z polarized ruby-laser light the generated Raman Stokes light was found to be polarized in the same direction. According to Eq. (1), this corresponds to Raman scattering from A_1 modes. In the notation of Porto[31] the scattering geometry is designated by $x(zz)x$. In Ref. 15 the slight deviation of the propagation direction of the laser light from the x direction towards the y direction is characterized by adding a term Δy, yielding $[x+\Delta y](zz)x$.

Figure 2(a) shows the measured threshold intensities I_{th} for SRS with the resonator (solid squares and triangles) as a function of temperature T. The accuracy of the absolute values of the threshold intensities is about $\pm 30\%$. The relative error of the measured temperature dependence of the threshold intensities is about $\pm 10\%$ (see error bars in the figures). The solid lines have been calculated from the measured spontaneous Raman data in the following way. The peak intensity I_0^{sp} in the center of the spontaneous Raman line was determined at various temperatures from the ratio of the frequency-integrated intensity I_{int}^{sp} to the linewidth $\delta\bar{\nu}_R$. It was assumed that the peak intensity I_0^{sp} is proportional to the peak scattering cross section $(d^2\sigma/d\omega\, d\Omega)_P$, the inverse of which determines the threshold intensity of SRS [see Eq. (3)]. The experimentally determined values of the inverse $1/I_0^{sp}$ of the spontaneous peak intensity at various temperatures were interpolated by a continuous curve, which is shown in the figures. Since the proportionality factor in Eq. (3) is not known, the curve was fitted at one definite temperature to the corresponding threshold intensity I_{th} of SRS for every Raman mode.

The procedure of calculating the threshold intensity of SRS from the spontaneous Raman data is illustrated for the 104-cm^{-1} zz A_1 mode. The measured spontaneous Raman linewidth $\delta\bar{\nu}_R$ (solid triangles) and the frequency-integrated spontaneous Raman intensity I_{int}^{sp} (open triangles) are plotted versus temperature T in Fig. 3. The Raman linewidth $\delta\bar{\nu}_R$ increases from 0.073 cm^{-1} at 10 K to 0.2 cm^{-1} at 40 K (scale on the left-hand side of Fig. 3). There is also an increase of the spontaneous Raman intensity I_{int}^{sp} (scale on the right-hand side) with rising temperature because of the increasing population of the phonon mode. The peak intensity I_0^{sp} of spontaneous Raman scattering is obtained by dividing the integrated spontaneous intensity I_{int}^{sp} by the spontaneous linewidth $\delta\bar{\nu}_R$.

Stimulated Raman scattering from the 104-cm^{-1} zz A_1 mode was observed for temperatures below 40 K. In this temperature range the integrated spontaneous Raman intensity I_{int}^{sp} is nearly constant. Therefore, the temperature dependence of the inverse $1/I_0^{sp}$ of the spontaneous peak intensity and of the threshold intensity I_{th} of SRS is determined by the temperature dependence of the spontaneous Raman linewidth $\delta\bar{\nu}_R$ [see Eq. (3)]. A comparison between the threshold intensities I_{th} for SRS [solid triangles in Fig. 2(a)] and the inverse of the spontaneous peak intensity, $1/I_0^{sp}$ (solid line), shows that the temperature dependence of I_{th} for this mode is described very well by the spontaneous Raman peak intensity $1/I_0^{sp}$. The good agreement is expected because the spontaneous Raman linewidths (see Fig. 3) are small compared with the laser linewidth over the investigated temperature range, but large enough for quasistationary SRS.

At temperatures above 40 K the threshold intensity I_{th} for SRS from the zz A_1 mode with a frequency shift of

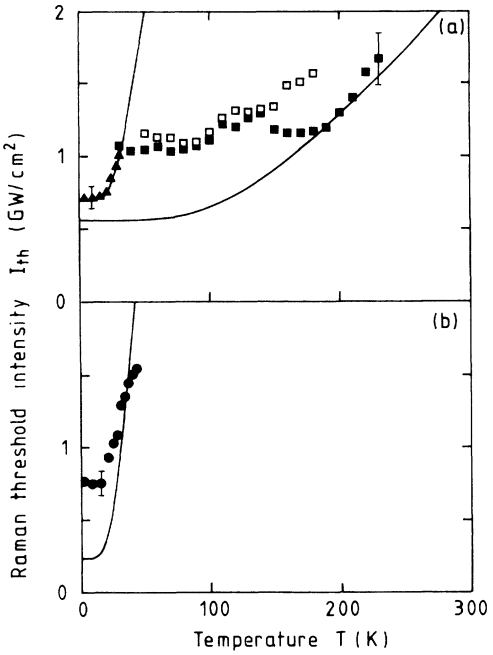

FIG. 2. Raman threshold intensity I_{th} vs temperature T. (a) $[x+\Delta y](zz)x$ configuration. The solid squares and triangles correspond to stimulated Raman scattering with resonator from the 1372- and 104-cm^{-1} zz A_1 modes, respectively. The open squares represent stimulated Raman scattering without resonator from the 1372-cm^{-1} zz A_1 mode. (b) $[x+\Delta z](yy)x$ configuration. The solid circles correspond to the 79-cm^{-1} yy A_1 mode. The solid lines are proportional to the inverse of the peak intensities in the center of the spontaneous Raman lines.

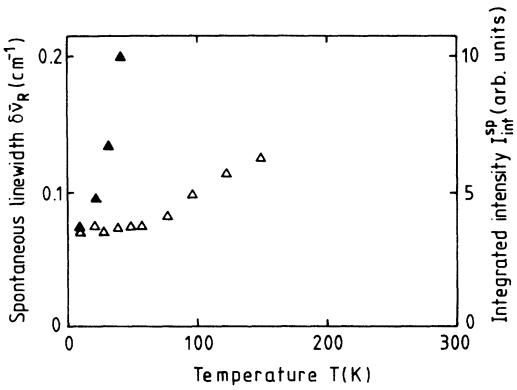

FIG. 3. Spontaneous Raman data of the 104-cm^{-1} zz A_1 mode. Spontaneous Raman linewidth $\delta\bar{\nu}_R$ (solid triangles, scale on the left-hand side) and frequency-integrated spontaneous Raman intensity I_{int}^{sp} (open triangles, scale on the right-hand side) vs temperature T.

1372 cm^{-1} [solid squares in Fig. 2(a)] is lower than that of the 104-cm^{-1} zz A_1 mode. The threshold intensity of the 1372-cm^{-1} mode decreases with decreasing temperature down to about 150 K and remains constant within the experimental accuracy at lower temperatures. There are deviations between the experimental points and the calculated curve. At low temperatures the spontaneous Raman data (solid line) are below the stimulated Raman results (solid squares).

For an explanation of this discrepancy we measured the threshold intensity for SRS from the 1372-cm^{-1} mode also *without* the Raman resonator. The data are shown as open squares in Fig. 2(a). At temperatures below 150 K the threshold intensities with and without the resonator are equal within the experimental accuracy. For $T > 150$ K the threshold intensities with the Raman resonator are lower than that without a resonator. In this temperature range the spontaneous Raman linewidth $\delta\bar{\nu}_R$ of the 1372-cm^{-1} zz A_1 mode is larger than 2 cm^{-1},[18] i.e., large compared to the laser linewidth $\delta\bar{\nu}_L \simeq 0.7$ cm^{-1}. Therefore, the full steady-state gain is expected to occur *both* in the forward and backward direction.[25,26] The feedback of the Raman resonator is effective and leads to the lower threshold intensities (solid squares). At temperatures below 150 K the spontaneous Raman linewidth $\delta\bar{\nu}_R$ approaches a value of 0.9 cm^{-1} which is close to the laser linewidth $\delta\bar{\nu}_L$. In this case, the critical intensities I_{cr} have to be considered. The critical intensity I_{cr}^{bw} for backward Raman scattering is rather high (see Sec. III). Therefore, the laser intensity I_L may not exceed I_{cr}^{bw}, yielding a reduced gain factor in the backward direction. Since the reflectivity of the resonator mirrors is not high (67%) for the 1372-cm^{-1} line, a small backward Raman gain reduces the feedback effect of the resonator mirrors strongly, leading to about equal threshold intensities for SRS with and without resonator.

The missing feedback below 150 K also explains the discrepancy at these temperatures between the measured threshold intensities for the 1372-cm^{-1} mode and the solid line calculated from the spontaneous Raman data. The solid line has been fitted to the high-temperature data of SRS, for which the Raman resonator is effective. Therefore, it lies below the SRS data at low temperatures, where the resonator is not effective.

2. *y polarized laser light*

We have also carried out experiments with the laser light polarized in the y direction (propagating close to the x direction). SRS was obtained from the yy A_1 mode with a frequency of about 79 cm^{-1} (geometry $[x+\Delta z](yy)x$), but only below 40 K. The threshold intensity first decreases steeply with decreasing temperature and then remains constant [solid circles in Fig. 2(b)]. The solid line calculated from the spontaneous peak intensity I_0^{sp} shows also a steep decrease with temperature T. However, it reaches much lower values than the solid circles obtained from SRS. We have measured also the threshold intensities without the Raman resonator and found that they are higher than those with resonator all over the investigated temperature range. For an explanation of the discrepancy between the calculated solid line and the experimental points it should be noted that the spontaneous Raman linewidth $\delta\bar{\nu}_R$ of the 79-cm^{-1} yy A_1 mode is less than 0.01 cm^{-1} at temperatures below 15 K, which is of the order of our spectral resolution.[18] For such narrow Raman linewidths SRS may already be transient, leading to a reduced Raman gain factor and a larger threshold intensity than that predicted by the steady-state theory.

For temperatures between 40 and 80 K stimulated Raman scattering from the 1375-cm^{-1} yy A_1 mode was observed. Since the Raman threshold intensities were close to the damage threshold intensity we have obtained only a few data points which are not shown in Fig. 2(b).

B. *y* direction

In this case, the axis of the Raman resonator was parallel to the y direction of the lithium formate monohydrate crystal. The propagation directions of the Stokes and laser light were close to the y direction.

1. *x polarized laser light*

In the investigated temperature range SRS was observed only from B_1 modes ($[y+\Delta z](xz)y$ geometry). From 130 to 50 K the 163-cm^{-1} B_1 mode was dominant [solid diamonds in Fig. 4(a)]. In the spontaneous Raman spectrum[18] this mode consists of two lines, which overlap strongly all over the investigated temperature range. In Fig. 4(a) we plotted the inverse of the spontaneous peak intensity I_0^{sp} at the frequency of the peak of the stronger of both Raman lines as solid line (1). There is good agreement with the experimental points (solid diamonds) for SRS.

Between 50 and 25 K stimulated Raman scattering was observed from the 113-cm^{-1} B_1 mode. The spontaneous Raman data of this mode are presented in Fig. 5. As expected, the spontaneous Raman linewidth $\delta\bar{\nu}_R$ (solid circles, scale on the left-hand side) and the frequency-

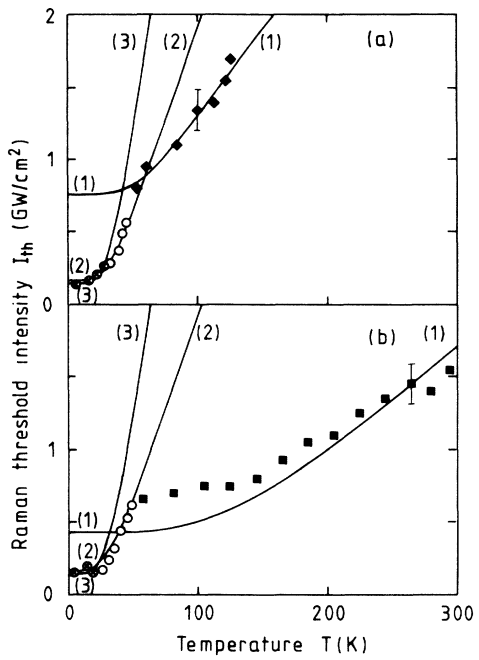

FIG. 4. Raman threshold intensity I_{th} vs temperature T. (a) The solid diamonds represent the 163-cm^{-1} B_1 mode and the open and crossed circles the 113- and 82-cm^{-1} B_1 modes, respectively ($[y+\Delta z](xz)y$ configuration). (b) The solid squares correspond to the 1372-cm^{-1} zz A_1 mode ($[y+\Delta x](zz)y$ configuration) and the open and crossed circles to the 113- and 82-cm^{-1} B_1 modes, respectively ($[y+\Delta x](zx)y$ configuration). The solid lines are proportional to the inverse of the peak intensities in the center of the spontaneous Raman lines.

integrated spontaneous Raman intensity I_{int}^{sp} (open circles, scale on the right-hand side) increase with rising temperature. In the temperature range from 25 to 50 K, which is relevant for SRS from this mode, the integrated Raman intensity is approximately constant. Therefore, the temperature dependence of the threshold intensity of SRS is determined by the spontaneous Raman linewidth $\delta\bar{\nu}_R$ [see Eq. (3)].

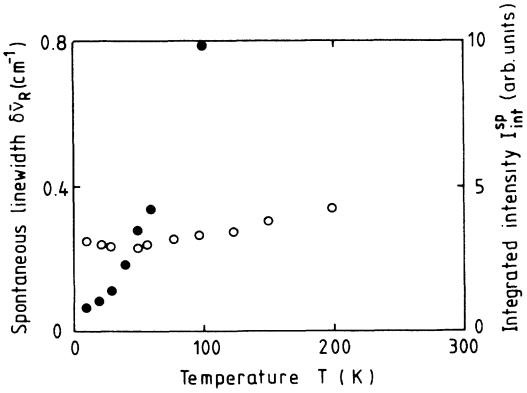

FIG. 5. Spontaneous Raman data of the 113-cm^{-1} B_1 mode. Spontaneous Raman linewidth $\delta\bar{\nu}_R$ (solid circles, scale on the left-hand side) and frequency-integrated spontaneous Raman intensity I_{int}^{sp} (open circles, scale on the right-hand side) vs temperature T.

It can be seen from Fig. 4(a) that below the temperature range (50 to 25 K) in which stimulated Raman scattering from the 113-cm^{-1} B_1 mode (open circles) was observed, the B_1 mode with a frequency of 82 cm^{-1} (crossed circles) was dominant. It should be emphasized, however, that the threshold intensities of these modes were so close to each other that sometimes both modes were observed simultaneously. The solid lines (2) and (3) were obtained from the spontaneous peak intensities I_0^{sp} of the 113- and 82-cm^{-1} B_1 modes, respectively, whose spontaneous Raman linewidths increase strongly with temperature,[18] but below 50 K are always much smaller than the laser linewidth (see, e.g., Fig. 5). The inverse values of the spontaneous peak intensities, $1/I_0^{sp}$, of the 82- and 113-cm^{-1} B_1 modes have a similar temperature dependence. However, the 82-cm^{-1} curve (3) starts below the 113-cm^{-1} curve (2) at low temperatures [difficult to see in Fig. 4(a) because of the experimental points] and exhibits a steeper rise than the 113-cm^{-1} curve (2) at higher temperatures. Therefore, for temperatures $T<25$ K stimulated Raman scattering is observed mainly from the 82-cm^{-1} mode (crossed circles), while between 25 and 50 K the 113-cm^{-1} mode (open circles) is dominant. The agreement between the experimental points for SRS and the solid lines representing the spontaneous Raman data is good.

2. *z polarized laser light*

The measured threshold intensity I_{th} for SRS versus temperature T for z polarized laser light propagating in the y direction (y-cut crystal) is shown in Fig. 4(b). From room temperature to 50 K we observed SRS from the 1372-cm^{-1} zz A_1 mode (solid squares) of lithium formate monohydrate ($[y+\Delta x](zz)y$ configuration) which corresponds to the strongest spontaneous Raman line at room temperature.[13] The temperature dependence of the threshold intensity in this y-cut crystal [Fig. 4(b)] is the same *within the experimental accuracy* as in the x-cut crystal [Fig. 2(a)] because the same Raman tensor element zz is involved. This can be seen best if the experimental points of the x- and y-cut crystals are normalized to the same height. However, the absolute values of I_{th} are lower for the y-cut crystal than for the x-cut crystal because the former had a longer length and a much better optical quality of the surfaces (see Sec. IV). The solid squares for SRS from the 1372-cm^{-1} mode deviate at lower temperatures from the solid line (1) representing the spontaneous Raman data [see Fig. 4(b)]. An explanation for this discrepancy has been given in Sec. V A 1.

At temperatures between 50 and 25 K and below 25 K stimulated Raman scattering from the 113- and 82-cm^{-1} B_1 modes, respectively, occurred in a similar way as discussed for the x polarized laser light [compare Figs. 4(a) and 4(b)]. The agreement between the points for SRS (open and crossed circles) and the solid lines (2) and (3) is good.

Overall, Figs. 4(a) and 4(b) show that below 10 K the threshold intensities of SRS from the 82-cm^{-1} B_1 mode are very small (<200 MW/cm^2) for the y-cut crystal, which has parallel surfaces of high optical quality.

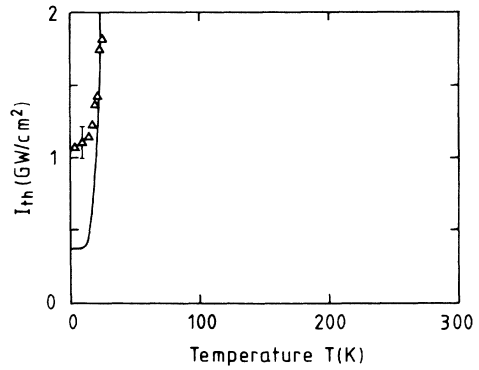

FIG. 6. Raman threshold intensity I_{th} vs temperature T. The open triangles correspond to the 76-cm^{-1} A_2 mode ($[z+\Delta y](xy)z$ configuration). The solid line is proportional to the inverse of the peak intensity in the center of the spontaneous Raman line.

Therefore, stimulated Raman scattering with high conversion efficiency is easily obtained without optical damage of the crystal.

C. z direction

When the axis of the Raman resonator was parallel to the z direction of the lithium formate monohydrate crystal, SRS was observed from the 76-cm^{-1} A_2 mode both for x and y polarized ruby-laser light, however only at temperatures below 40 K. The results for the $[z+\Delta y](xy)z$ geometry are shown in Fig. 6. Similar results have been obtained for the $[z+\Delta x](yx)z$ geometry. The threshold intensity I_{th} for SRS decreases steeply with decreasing temperature and reaches a constant value for low temperatures.

The inverse of the spontaneous Raman peak intensity (solid line) of the 76-cm^{-1} A_2 mode shows also a steep decrease, but reaches much lower values for $T<20$ K than I_{th}. The reason for this discrepancy is the very small spontaneous Raman linewidth $\delta\bar{\nu}_R$ (much smaller than 10^{-2} cm^{-1} for $T<20$ K) of this mode[18] which causes a transient behavior of SRS and rises the threshold intensity I_{th} above the solid line obtained from the spontaneous Raman data for the steady-state case.

VI. CONCLUSIONS

We have investigated stimulated Raman scattering in lithium formate monohydrate single crystals in a resonator configuration for various propagation directions in the crystal and for different polarizations of the laser light from 2 K to room temperature. The pump laser was a Q-switched ruby laser with a linewidth of 0.7 cm^{-1}. For our particular experimental conditions the following results were obtained. For temperatures above about 50 K the zz A_1 mode with a frequency of 1372 cm^{-1} and the 163-cm^{-1} B_1 mode had the lowest threshold intensities for stimulated Raman scattering. At temperatures below 50 K stimulated Raman scattering was observed only from low-frequency modes, in particular from the 104-cm^{-1} zz and the 79-cm^{-1} yy A_1 modes, the 76-cm^{-1} A_2 mode, and the 82- and 113-cm^{-1} B_1 modes.

We have also measured the spontaneous widths and intensities of those Raman lines[18] which have been observed in stimulated Raman scattering. The spontaneous Raman linewidths range from <0.01 to 13 cm^{-1} depending on the lattice mode and the temperature. The dominance of the low-frequency modes in stimulated Raman scattering at low temperatures is due to the small linewidths of the corresponding spontaneous Raman lines, which lead to high spontaneous Raman peak intensities. In the steady-state case, the threshold intensity for SRS is proportional to the inverse of the spontaneous Raman peak intensity, i.e., high spontaneous peak intensities cause low threshold intensities for SRS. This relation has been confirmed for the 104-cm^{-1} zz A_1 mode and the 82-, 113-, and 163-cm^{-1} B_1 modes. Deviations between the spontaneous and stimulated Raman data were found for the 76-cm^{-1} A_2 mode and the 79-cm^{-1} yy A_1 mode. These modes have extremely narrow ($<10^{-2}$ cm^{-1}) spontaneous Raman lines at low temperatures, which give rise to transient stimulated Raman scattering resulting in a reduced Raman gain and an increased threshold intensity compared with the steady-state case. Stimulated Raman scattering from the 1372-cm^{-1} zz A_1 mode was a particular case, because the feedback by the Raman resonator was fully effective only at higher temperatures, but not at low temperatures ($T<150$ K). This has been explained by taking into account the temperature dependence of the ratio of the spontaneous Raman linewidth and the ruby-laser linewidth.

Since the $A_1(z)$ and $B_1(x)$ modes are both Raman and ir active, the excitation of these modes by stimulated Raman scattering can be used to generate intense, monochromatic, coherent far-infrared and ir light pulses at the investigated frequencies (79, 82, 104, 113, 163, and 1372 cm^{-1}). In addition, high population numbers of optical phonons are produced, which decay into acoustic phonons with terahertz frequencies. Stimulated Raman scattering may serve, therefore, as a source of high-frequency acoustic phonons.

*Present address: Inorganic Chemistry Laboratory, University of Oxford, Oxford, UK.

†Present address: Institut für Physikalische und Theoretische Chemie, Universität Erlangen, D-8520 Erlangen, FRG.

[1]A. L. Aleksandrovskii, A. N. Izrailenko, and L. N. Rashkovich, Kvantovaya Elektron (Moscow) **1**, 1261 (1974) [Sov. J. Quantum Electron. **4**, 699 (1974)].

[2]J. Szewczyk, J. Karniewicz, and W. Kolasinski, J. Cryst. Growth **60**, 14 (1982).

[3]H. Pykacz, Acta Phys. Pol. A **55**, 855 (1979).

[4]H. Veeser, U. Bogner, and W. Eisenmenger, Phys. Status Solidi A **37**, 161 (1976).

[5]S. J. Bastow and M. H. Dunn, Opt. Commun. **35**, 259 (1980); V. I. Stroganov, B. I. Kidyarov, and V. I. Trunov, Opt. Spectrosc. **47**, 319 (1979); V. I. Stroganov, V. I. Trunov, A. A. Chernenko, and A. N. Izrailenko, Kvantovaya Elektron.

(Moscow) **3**, 1122 (1976) [Sov. J. Quantum Electron. **6**, 601 (1976)]; F. B. Dunning, F. K. Tittel, and R. F. Stebbings, Opt. Commun. **7**, 181 (1973).

[6]S. Singh, W. A. Bonner, J. R. Potopowicz, and L. G. Van Uitert, Appl. Phys. Lett. **17**, 292 (1970).

[7]K. Kato, Opt. Quantum Electron. **8**, 261 (1976).

[8]S. A. Akhmanov, A. N. Dubovik, S. M. Saltiel, I. V. Tomov, and V. G. Tunkin, Pis'ma Zh. Eksp. Teor. Fiz. **20**, 264 (1974) [JETP Lett. **20**, 117 (1974)].

[9]R. B. Andreev, V. D. Volosov, and L. I. Kuznetsova, Kvantovaya Elektron. (Moscow) **2**, 420 (1975) [Sov. J. Quantum Electron. **5**, 242 (1975)].

[10]R. N. Gyuzalyan, D. G. Sarkisyan, and M. L. Ter-Mikaelyan, Kvantovaya Elektron. (Moscow) **4**, 1138 (1977) [Sov. J. Quantum Electron. **7**, 645 (1977)].

[11]P. V. Avizonis, F. A. Hopf, W. D. Bomberger, S. F. Jacobs, A. Tomita, and K. H. Womack, Appl. Phys. Lett. **31**, 435 (1977).

[12]Yu. N. Polivanov and K. A. Prokhorov, Fiz. Tverd. Tela (Leningrad) **22**, 1360 (1986) [Sov. Phys.—Solid State **22**, 768 (1980)]; M. Cadene, C. R. Séances, Acad. Sci. (Paris) Ser. B **270**, 909 (1970); R. S. Krishnan and P. S. Ramanujan, Indian J. Pure Appl. Phys. **9**, 910 (1971).

[13]J. C. Galzerani, R. Srivastava, R. S. Katiyar, and S. P. S. Porto, J. Raman Spectrosc. **6**, 174 (1977).

[14]O. A. Doil'nitsyna, Yu. N. Polivanov, and K. A. Prokhorov, Kvantovaya Elektron. (Moscow) **8**, 2268 (1981) [Sov. J. Quantum Electron. **11**, 1389 (1981)]; Yu. N. Polivanov and K. A. Prokhorov, Fiz. Tverd. Tela (Leningrad) **21**, 3593 (1979) [Sov. Phys.—Solid State **21**, 2074 (1979)]; M. Yamamoto, H. Ito, and H. Inaba, Phys. Lett. **55a**, 303 (1975).

[15]L. I. Kuznetsova, L. A. Kulevskii, Yu. N. Polivanov, and K. A. Prokhorov, Kvantovaya Elektron. (Moscow) **2**, 2095 (1975) [Sov. J. Quantum Electron. **5**, 1146 (1975)].

[16]O. A. Aktsipetrov, G. Kh. Kitaeva, and A. N. Penin, Fiz. Tverd. Tela (Leningrad) **19**, 127 (1977) [Sov. Phys.—Solid State **19**, 72 (1977)].

[17]A. T. Sukhodol'skii, Pis'ma Zh. Eksp. Teor. Fiz. **27**, 185 (1978) [JETP Lett. **27**, 173 (1978)].

[18]M. Jordan, H.-J. Jodl, and M. Maier, Chem. Phys. (to be published).

[19]A. Enders-Beumer and S. Harkema, Acta Crystallogr. Sect. B **29**, 682 (1973); J. K. Mohana Rao and M. A. Viswamitra, Ferroelectrics **2**, 209 (1971).

[20]V. I. Yuzvak, L. I. Kuznetsova, I. S. Rez, and I. P. Aleksandrova, Kristallografiya **22**, 106 (1977) [Sov. Phys. Crystallogr. **22**, 59 (1977)].

[21]R. Loudon, Adv. Phys. **13**, 423 (1964).

[22]A. Anderson, *The Raman Effect* (Dekker, New York, 1973), p. 834.

[23]W. Kaiser and M. Maier, in *Laser Handbook,* edited by F. T. Arecchi and E. O. Schulz-Dubois (North-Holland, Amsterdam, 1972), Vol. 2, p. 1077.

[24]S. A. Akhmanov, Yu. E. D'yakov, and L. I. Pavlov, Zh. Eksp. Teor. Fiz. **66**, 520 (1974) [Sov. Phys.—JETP **39**, 249 (1974)].

[25]I. G. Zubarov and S. I. Mikhailov, Kvantovaya Elektron. (Moscow) **5**, 2383 (1978) [Sov. J. Quantum Electron. **8**, 1338 (1978)].

[26]W. R. Trutna, Y. K. Park, and R. L. Byer, IEEE J. Quantum Electron. **QE-15**, 648 (1979).

[27]M. G. Raymer, J. Mostowski, and J. L. Carlsten, Phys. Rev. A **19**, 2304 (1979).

[28]H. Naito and H. Inaba, Opto-Electron. **5**, 256 (1973).

[29]M. G. Raymer and J. Mostowski, Phys. Rev. A **24**, 1980 (1981); I. M. Bel'dyugin, M. V. Zolotarev, and K. A. Sviridov, Kvantovaya Elektron. (Moscow) **12**, 208 (1985) [Sov. J. Quantum Electron. **15**, 133 (1985)].

[30]A. S. Pine and P. E. Tannenwald, Phys. Rev. **178**, 1424 (1969).

[31]D. A. Long, *Raman Spectroscopy* (McGraw-Hill, New York, 1977), p. 64.